Research Article

Engineering Beauty Molecules: Computational Validation of Osthole Derivatives for Fragrance, Antioxidant, Anti-Melanogenic and Anti-Inflammatory Cosmeceutical Applications

D Divya, A Kalpana*

PG & Research Department of Chemistry, Sri Sarada College for Women, (Affiliated to Periyar University), Salem 636 016, Tamil Nadu, India.

***Corresponding author's E-mail:** kalpanaanbarasu@gmail.com

Received: 04-05-2026; **Revised:** 22-07-2026; **Accepted:** 29-07-2026; **Published online:** 20-08-2026.

ABSTRACT

This study provides a robust computational framework for the validation of osthole-based derivatives as multifunctional agents with promising roles in fragrance, antioxidant, anti-melanogenic and anti-inflammatory cosmeceutical applications. ADMET profiling indicated that most derivatives possess favorable cosmetic-likeness, skin permeability and non-toxicity. Molecular docking analysis revealed that ester derivatives exhibited strong antioxidant and anti-inflammatory activities, while maintaining good fragrance receptor affinity. Oxime-based derivatives showed enhanced antioxidant and anti-inflammatory binding, whereas hydrazone derivatives demonstrated superior anti-inflammatory and anti-melanogenic potential. Amide derivatives displayed a well-balanced multitarget profile across all activities. SAR analysis highlighted that optimal chain length, electron-withdrawing substituents and conjugated or heterocyclic systems significantly enhance binding affinity, while amide and oxime linkages improve hydrogen-bonding capacity and target adaptability. Overall, the analysis revealed that ester derivatives were most effective for fragrance and antioxidant activity, oxime and hydrazone derivatives for anti-inflammatory and anti-melanogenic effects and amide derivatives for balanced multifunctional performance.

Keywords: Anti-inflammatory agents, Anti-melanogenic agents, Antioxidants, Cosmeceutical applications, Fragrant compounds, Osthole derivatives.

GRAPHICAL ABSTRACT

In silico validation of osthole derivatives as cosmeceuticals

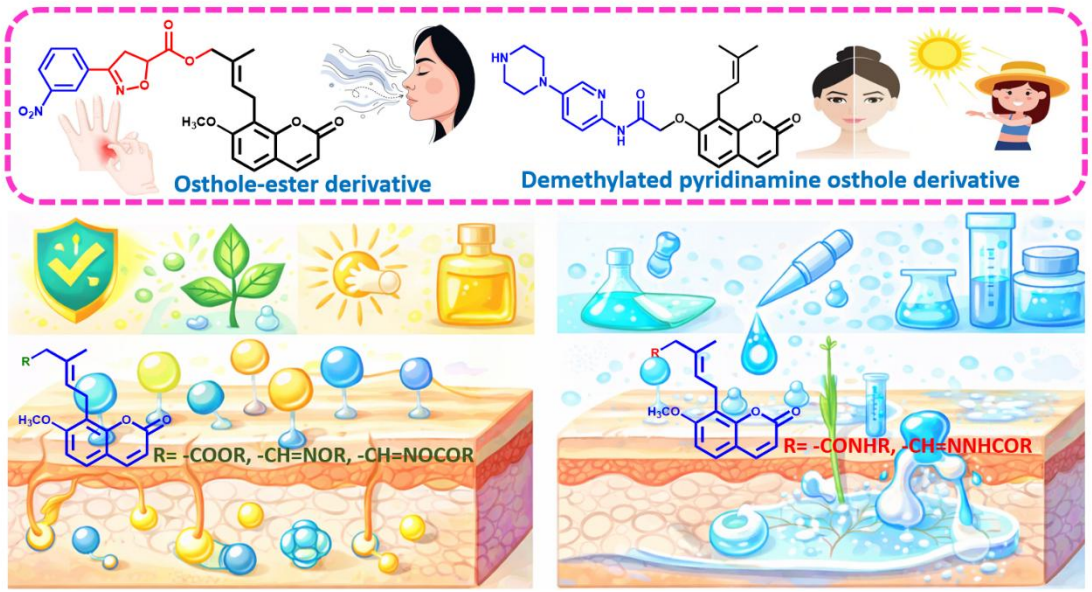

INTRODUCTION

Coumarins constitute a prominent class of naturally occurring phytochemicals known for their broad spectrum of bioactivities including antioxidant, anti-inflammatory, antimicrobial, photoprotective and melanogenesis-regulating effects, which underpin their growing relevance in cosmeceutical development. Osthole, a major bioactive constituent of *Cnidium monnieri*, has attracted significant attention as a multifunctional skin-active molecule. Experimental evidence indicates that osthole effectively attenuates oxidative stress, protects tissues from inflammation-induced damage and suppresses melanogenesis *via* down-regulation of tyrosinase and related proteins.[1]

In silico analysis provides a rapid, cost-effective and predictive approach to evaluate molecular properties, biological activity and safety profiles[2], thereby accelerating early-stage drug and cosmeceutical development. Based on this rationale, a series of osthole-ester (**1a-1c**), -amide (**2**), -oxime-ether (**3**)/ester (**4**), -acylhydrazone (**5**), -

©Copyright protected. Unauthorised republication, reproduction, distribution, dissemination and copying of this document in whole or in part is strictly prohibited.

demethylated amide/amine/piperazine/pyridinamine (**6**) analogues[3] (Figure 1) were selected in the present study to systematically evaluate their dermato-pharmacokinetic properties and multifunctional cosmetic activities including fragrance, antioxidant, anti-melanogenic, and anti-inflammatory effects through integrated molecular docking and ADMET analyses, with the objective of identifying novel lead compounds that exhibit enhanced efficacy and improved skin compatibility.

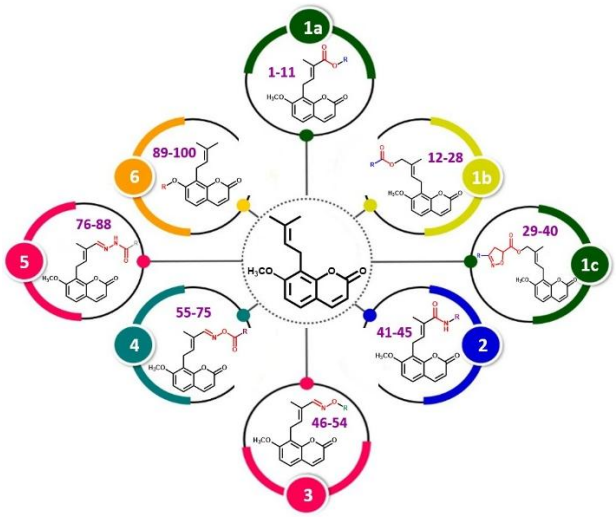

Figure 1: Osthole derivatives.

Molecular docking was performed against key protein targets relevant to cosmetic bioactivity, including human olfactory receptor (OR51E2), Kelch-like ECH-associated protein 1 (Keap1- cellular redox-sensing regulatory protein), human tyrosinase (initiates and regulates melanin biosynthesis), prostaglandin G/H synthase (cyclooxygenase).

MATERIALS AND METHODS

The geometrical structures of the osthole derivatives and reference compounds were optimized using the Chem3D software employing the MM2 force field. The crystal structures of OR51E2 (PDB ID: 8F76), Keap1 (PDB ID: 6TYM), Tyrosinase (PDB ID: 2Y9X) and COX-2 (PDB ID: 3LN1) were obtained from the Protein Data Bank. Prior to docking, the protein structures were prepared by removing all bound ligands, cofactors and water molecules. Molecular docking simulations were performed using AutoDock Tools.[4] The resulting docking poses and key ligand-protein interactions were visualized and analyzed using UCSF Chimera[5] and BIOVIA Discovery Studio Visualizer.[6] Furthermore, the ADMET properties were predicted using the SwissADME and DeepPKCSM web servers.[7,8]

RESULTS AND DISCUSSION

Pharmacokinetics and safety profiling of osthole derivatives

The structural details of the osthole derivatives, including compound numbers, IUPAC names, 2D structures, binding energy, ADMET parameters and safety profiles are presented in Supplementary Table S1 and Table S2. A comprehensive ADME-toxicity assessment of osthole derivatives (**1-100**) revealed a well-balanced physicochemical and safety profile, supporting their potential as multifunctional cosmetic actives. Across all series, compounds exhibited moderate aqueous solubility and optimal lipophilicity (iLogP: 2.80-4.29), facilitating efficient interaction with the lipid-rich stratum corneum. Skin permeability values (log Kp: -4.75 to -6.59 cm/s), in conjunction with TPSA (61.03-133.15 Å²), indicated an appropriate polarity-lipophilicity balance conducive to controlled dermal absorption and retention. Uniform bioavailability scores (0.55) and low-to-moderate synthetic accessibility (3.38-4.74) further confirm favorable drug-like disposition and practical synthetic feasibility throughout the series. Notably, all compounds obey Lipinski rule of five.

Series-wise analysis demonstrated that ester derivatives (**1-40**) possess relatively higher lipophilicity (3.12-4.22) and permeability, favouring enhanced skin deposition and barrier affinity. In contrast, amide derivatives (**41-45**) exhibited improved polarity (TPSA: 68.54-87 Å²) and strict compliance with Lipinski, Ghose, Veber, Egan, and Muegge criteria, suggesting predictable dermal kinetics and superior formulation stability. Oxime-ether (**46-54**) and oxime-ester (**55-75**) derivatives showed consistent physicochemical parameters (iLogP ~3.9-4.29; log Kp ~-5.14 to -5.67 cm/s), promoting efficient stratum corneum partitioning and prolonged topical retention, with oxime-esters representing the most structurally uniform subset. Acylhydrazone derivatives (**76-88**) maintained comparable lipophilicity and permeability, while the incorporation of hydrazone functionality enhanced polarity (TPSA: 80.9-126.72 Å²), supporting controlled dermal transport. Notably, nitrogen-enriched derivatives (**89-100**) exhibited the widest physicochemical variability, characterized by lower lipophilicity (iLogP: 2.80-3.75) and broader permeability distribution, indicative of enhanced solubility and faster dermal release. Although minor deviations from Ghose and Muegge criteria were observed in select pyridinamine analogs, overall drug-likeness compliance remained satisfactory. Importantly, all derivatives demonstrated favorable safety profiles, with no predicted eye corrosion and eye irritation and were further characterized as non-skin sensitizing, biodegradable and non-carcinogenic.

The structure-cosmetic function relationship analysis revealed that lipophilicity and polarity play a crucial role in determining dermal performance and formulation suitability of the derivatives. Compounds with higher lipophilicity, such as ester, oxime-ether, and oxime-ester derivatives, exhibit enhanced skin deposition and retention, making them well-suited for barrier-protective, antioxidant, UV-protective and fragrance-fixative applications. In contrast, derivatives with balanced polarity, including amides and hydrazones, demonstrate predictable skin penetration along with improved stability, supporting their use in general dermatological and anti-aging formulations. Meanwhile, nitrogen-rich derivatives with higher polarity show improved aqueous solubility and relatively faster dermal release, rendering them particularly suitable for

©Copyright protected. Unauthorised republication, reproduction, distribution, dissemination and copying of this document in whole or in part is strictly prohibited.

hydrophilic cosmetic systems such as serums and gels. Collectively, the integration of optimal lipophilicity, controlled permeability and robust safety profiles highlights these osthole derivatives as promising candidates for advanced cosmetic formulations, particularly for applications requiring antioxidant activity, UV protection, fragrance fixation and skin barrier enhancement.

Docking-based evaluation of binding interactions

Osthole ester derivatives

Simple terminal esters (**1-11**) showed moderate-strong fragrance (-7.69 to -8.54 kcal/mol) and balanced dermato-protective activities (antioxidant -9.98 to -11.49; anti-melanogenic -7.23 to -8.20; anti-inflammatory -7.18 to -8.85 kcal/mol). Among the series, compounds **5, 2** and **3** emerged as the top multifunctional candidates (Figure 2). The SAR of the ester-linked osthole derivatives demonstrates that both side-chain length and aromatic substitution critically influence multitarget activity. Progressive elongation of the alkyl linker from benzyl (**1**, -CH_2Ph) to propyl **3** enhances fragrance affinity (-7.84 to -8.54 kcal/mol), indicating improved hydrophobic interaction with the olfactory receptor. However, excessive extension (**4**, -$(CH_2)_4$Ph) reduces overall activity, suggesting steric hindrance and suboptimal fitting within binding pockets. Introduction of unsaturation **5** yields the best overall profile, particularly for antioxidant and anti-melanogenic activities, highlighting the importance of conjugation and rigidity in stabilizing ligand-target interactions. In contrast, branched substitution (**6**, -CH(CH_3)-Ph) slightly improves anti-melanogenic activity but reduces anti-inflammatory affinity, indicating that steric bulk near the linkage can limit proper orientation. Substituent effects on the aromatic ring further refine activity, electron-withdrawing groups such as Cl (**9**) and Br (**10**) enhance anti-melanogenic and anti-inflammatory interactions, increased hydrophobic and halogen bonding contributions, whereas strongly withdrawing CF_3 **11** favours anti-melanogenic activity but slightly compromises fragrance binding. Meanwhile, electron-donating substitution (**7**, -CH_3) shows comparatively weaker activity, suggesting reduced interaction efficiency.

Relocation of esterification to the distal prenyl terminus (**12-28**) broadened activity ranges and enhanced potency (fragrance -7.18 to -9.69; antioxidant -10.11 to -12.08; anti-melanogenic -7.28 to -8.85; anti-inflammatory -7.11 to -9.40 kcal/mol), reflecting improved steric reach and lipophilic accommodation within diverse binding pockets. Within the series, compounds **25, 22, 23, 16** and **27** emerged as leading multifunctional candidates (Figure 2). The SAR of this series highlights the significant role of aromatic substitution, linker type and heterocyclic incorporation in modulating multitarget activity. Direct phenyl substitution **12** provides a balanced baseline, while halogen substitution enhances activity, particularly *p*-Cl **16**, which exhibits superior binding across all targets, indicating that electron-withdrawing groups improve hydrophobic and polar interactions. The *m*-Cl derivative **15** also shows strong activity, though slightly lower than the *p*-analogue, suggesting positional effects on binding orientation. Fluoro-substituted derivatives **13**, **14** maintain good antioxidant activity but comparatively reduced anti-melanogenic and anti-inflammatory interactions, indicating weaker electronic influence than chloro groups. In contrast, electron-donating groups such as *p*-CH_3 (**17**) and OCH_3 **18**, **19** provide moderate activity, suggesting that increased electron density slightly reduces binding efficiency. Introduction of a methylene spacer (**20-22**) alters flexibility and orientation. Notably, the *p*-NO_2 derivative **22** shows the highest fragrance and anti-inflammatory affinities, highlighting the strong impact of highly electron-withdrawing substituents. Incorporation of unsaturation **23** improves anti-melanogenic binding, confirming the beneficial role of conjugation and rigidity. Heterocyclic systems further enhance activity, benzo[d] [1,3] dioxole **25** exhibits the strongest antioxidant, high anti-melanogenic and anti-inflammatory affinities, indicating that fused oxygen-containing rings favor multiple interactions. Similarly, dioxine derivatives **27**, **28** show improved anti-inflammatory activity (up to -8.90 kcal/mol), suggesting enhanced steric complementarity and H-bonding capacity.

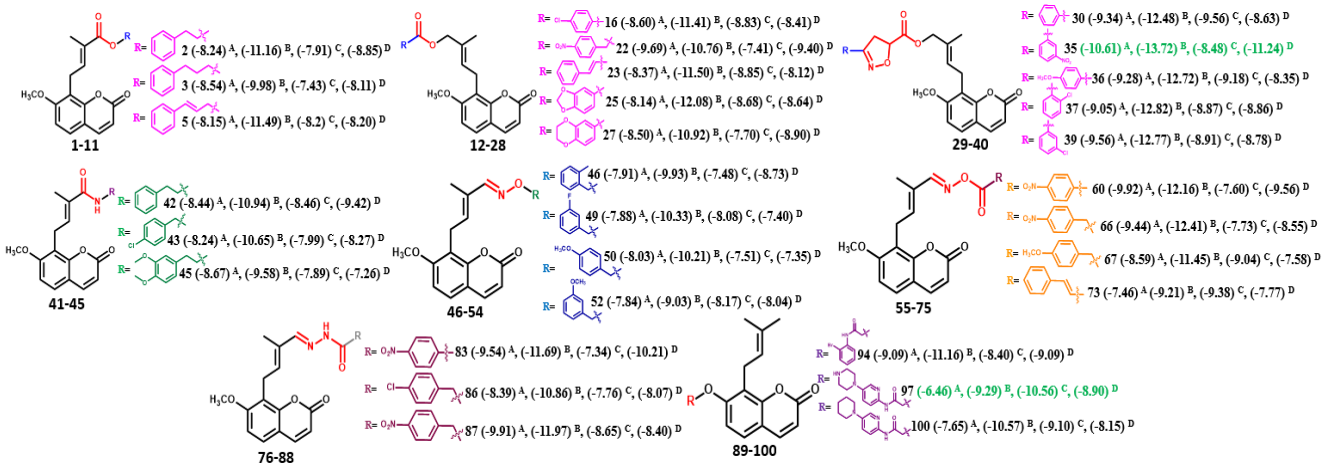

Figure 2: Active osthole derivatives and associated binding energies (A-fragrance, B-antioxidant, C-anti-melanogenic, D-anti-inflammatory activities).

©Copyright protected. Unauthorised republication, reproduction, distribution, dissemination and copying of this document in whole or in part is strictly prohibited.

The introduction of a heterocyclic N-O-linked ester spacer (**29-40**) produced the highest affinities of the series (fragrance -8.82 to -10.61; antioxidant -11.81 to -13.72; anti-melanogenic -6.99 to -9.56; anti-inflammatory -7.79 to -11.24 kcal/mol), consistent with increased conformational adaptability and additional polar interaction capacity. Within the series, compounds **35, 30, 36, 37** and **39** were identified as leading multifunctional candidates (Figure 2). The SAR of this series reveals that electron-withdrawing substituents and heteroaromatic incorporation significantly enhance multitarget activity. The unsubstituted phenyl derivative **30** shows strong baseline binding, particularly for anti-melanogenic activity, indicating efficient core-target complementarity. Introduction of halogen substituents (**29**, **32**, **34**, **37**, **39**) further improves antioxidant and anti-inflammatory interactions, with *o*- and *m*-substitutions providing better overall balance than *p*-analogues, suggesting positional effects on optimal binding orientation. Strong electron-withdrawing nitro groups exert the most pronounced influence, where *m*-NO_2 **35** demonstrates superior multitarget activity due to its ability to engage in complementary polar and non-polar interactions across targets. H-bonding ensures stable anchoring in all binding sites, while π-based interactions (π-lone pair, π-alkyl) and alkyl contacts enhance hydrophobic accommodation. The presence of the electron withdrawing -NO_2 group optimizes electron distribution, strengthening both electrostatic and van der Waals interactions. In the human olfactory receptor, these interactions support strong fragrance binding, while in the Keap1 antioxidant protein, additional π-lone pair and alkyl interactions further stabilize the complex. In COX-2, sulfur-x and π-alkyl interactions improve compatibility with the hydrophobic active site, collectively explaining its strong fragrance, antioxidant and anti-inflammatory activity (Figure 3). In contrast, *p*-NO_2 **31** shows excellent anti-inflammatory activity (-10 kcal/mol) but reduced anti-melanogenic binding, indicating positional sensitivity of substituent effects. Electron-donating groups such as *p*-CH_3 **33** and *p*-OCH_3 **36** maintain good activity, with methoxy substitution **36** notably improving anti-melanogenic affinity, due to additional hydrogen-bonding and π-electron interactions. Replacement with a heteroaromatic ring (thiophene, **40**) retains strong antioxidant and anti-inflammatory activity, suggesting that sulfur-containing rings can effectively mimic phenyl interactions while contributing additional electronic diversity.

Osthole amide derivatives

The derivatives (**41-45**) demonstrated moderate olfactory receptor binding (-7.09 to -8.67 kcal/mol) with sustained antioxidant interactions (-9.58 to -10.94 kcal/mol), while anti-melanogenic (-7.50 to -8.46 kcal/mol) and anti-inflammatory (-6.85 to -9.42 kcal/mol) affinities remained within an effective dermato-functional range. Within this subset, compounds **42**, **43** and **45** emerged as the principal multifunctional contributors (Figure 2). The SAR of the amide-linked osthole derivatives indicates that variation in the aromatic R-substituent significantly influences multitarget activity. Extension of the side chain from benzyl (**41**, R=CH_2Ph) to phenethyl **42** markedly improves all activities, particularly antioxidant and anti-inflammatory, suggesting that increased chain length enhances flexibility and optimal positioning of the aromatic ring within binding pockets. **42** exhibits a highly optimized profile, where its amide-linked aromatic extension enables diverse π-interactions and H-bonding, ensuring strong stabilization across all four targets. Substitution on the phenyl ring further modulates activity, the *p*-chloro derivative **43** maintains strong overall binding, indicating that electron-withdrawing groups favor interaction, through enhanced hydrophobic and dipolar contacts. In contrast, the *p*-methoxy derivative **44** shows reduced activity, implying that single electron-donating substitution may disrupt optimal binding orientation. However, the di-methoxy derivative **45** restores fragrance affinity, suggesting that multiple electron-donating groups can improve aromatic interactions, enhanced π-π stacking and H-bonding.

Osthole oxime-ether derivatives

Docking investigation of oxime-ether functionalized osthole derivatives (**46-54**), in which the prenyl side chain is transformed into an N-O-alkyl oxime ether, indicated a stable multitarget cosmeceutical activity. The series displayed a relatively narrow fragrance affinity window (-7.83 to -8.10 kcal/mol) and moderate antioxidant interactions (-9.01 to -10.33 kcal/mol), while anti-melanogenic (-7.48 to -8.17 kcal/mol) and anti-inflammatory (-7.15 to -8.73 kcal/mol) activities remained consistently within dermato-relevant ranges. Within the set, compounds **46, 49, 50** and **52** represented the most effective multifunctional members (Figure 2). The SAR of oxime-ether derivatives indicates that aromatic substitution on the oxime-linked side chain and substituent position play key roles in modulating activity. Methyl-substituted derivatives (**46-48**) show comparable fragrance and antioxidant profiles, with the *o*-analogue **46** exhibiting enhanced anti-inflammatory activity, suggesting that proximal steric bulk may favor π-cation and π-sulfur interactions with COX-2. Introduction of methoxy groups **49**, **50** improves antioxidant and anti-melanogenic activity, particularly for the *m*-substituted derivative **49**, indicating that electron-donating groups capable of H-bonding and π-lone pair interactions in Keap1 and COX-2, enhancing antioxidant and anti-inflammatory selectivity. Fluoro-substituted derivatives (**51-53**) display balanced activity across all targets, with *m*-fluoro **52** showing the highest anti-melanogenic affinity and improved anti-inflammatory interaction, suggesting favorable electronic and positional effects. In contrast, the strong electron-withdrawing cyano group **54** slightly reduces overall activity, indicating that excessive polarity may limit optimal binding.

Osthole oxime-ester derivatives

Docking studies of oxime-ester modified osthole derivatives (**55-75**), incorporating an N-O-acyl functionality on the prenyl side chain, revealed a broad yet coherent multitarget cosmeceutical activity spectrum. The series spanned wide fragrance affinities (-6.74 to -9.92 kcal/mol) and antioxidant

©Copyright protected. Unauthorised republication, reproduction, distribution, dissemination and copying of this document in whole or in part is strictly prohibited.

interactions (-7.52 to -12.41 kcal/mol), accompanied by substantial anti-melanogenic (-7.14 to -9.38 kcal/mol) and anti-inflammatory (-6.85 to -9.56 kcal/mol) activities. Within this group, compounds **60, 66, 67** and **73** represented the most prominent multifunctional derivatives (Figure 2). The SAR of this series highlights the influence of electronic effects, linker flexibility and heteroaromatic substitution on multitarget activity. The unsubstituted phenyl derivative **55** provides a moderate baseline, while *p*-substituted analogues reveal clear trends, electron-withdrawing groups, particularly *p*-NO_2 **60**, significantly enhance activity across all targets and achieves superior binding across OR51E2, Keap1 and COX-2 due to high interaction diversity (H-bonding, π-electronic, hydrophobic contacts). Similarly, *p*-Br **59** improves overall binding compared to lighter halogens, whereas *p*-F **58** shows moderate enhancement. In contrast, strongly withdrawing CF_3 **61** reduces activity, suggesting excessive polarity may hinder optimal binding. Electron-donating substitution (**62**, *p*-OCH_3) favours anti-melanogenic activity (-8.54 kcal/mol), indicating a role in stabilizing enzyme interactions. Introduction of a methylene spacer (**63-67**) improves flexibility and generally enhances binding, with *p*-NO_2 **66** and *p*-Cl **64** derivatives showing strong antioxidant and anti-inflammatory, while *p*-OCH_3 **67** yields the highest anti-melanogenic affinity. Heteroaromatic pyridine derivatives (**68-72**) exhibit moderate activity, suggesting that nitrogen incorporation provides additional polarity but may reduce hydrophobic interactions compared to phenyl analogues. Incorporation of unsaturation (**73-75**) improves anti-melanogenic activity, particularly for **73**, highlighting the beneficial effect of conjugation, although excessive modification **75** reduces antioxidant potency.

Osthole acylhydrazone derivatives

Docking evaluation of hydrazone-linked osthole derivatives (**76-88**), characterized by incorporation of an acylhydrazone (-C=N-NH-COR) functionality on the prenyl side chain, demonstrated a diversified multitarget cosmeceutical interaction profile. The series covered broad fragrance affinities (-6.63 to -9.91 kcal/mol) and strong antioxidant binding (-9.03 to -11.97 kcal/mol), together with moderate anti-melanogenic (-7.34 to -8.65 kcal/mol) and anti-inflammatory (-7.13 to -10.21 kcal/mol) activities. The strongest multifunctional performance in this group of analogues was observed for compounds **83**, **87** and **86** (Figure 2). The SAR of hydrazone-linked derivatives highlights the importance of electronic effects and side-chain extension in governing multitarget activity. The unsubstituted phenyl derivative **76** provides a moderate baseline, while electron-donating groups such as *p*-CH_3 **77** enhance anti-melanogenic activity (-8.44 kcal/mol), whereas *p*-OCH_3 **78** slightly reduces overall binding, indicating limited contribution of strong electron donation. In contrast, halogen substitution (**79-82**) improves activity, with *m*-F **80** and *p*-Br **82** showing enhanced anti-melanogenic affinity, suggesting favorable hydrophobic and electronic interactions. The most pronounced effect is observed with strong electron-withdrawing NO_2 groups, where *p*-NO_2 **83** significantly increases fragrance, antioxidant and anti-inflammatory activities and relies more on electrostatic π-cation interactions, favouring COX-2 binding. Introduction of a methylene spacer (**85-88**) further improves flexibility and binding orientation. Notably, CH_2-*p*-NO_2 **87** exhibits the highest overall activity across all targets, confirming the combined benefit of chain extension and strong electron-withdrawing substitution and displays enhanced adaptability across all targets, particularly strong interaction with tyrosinase through π-π, π-alkyl, π-sigma and H-bonding networks. Additionally, the naphthalene derivative **88** shows improved anti-melanogenic and anti-inflammatory activity, highlighting the role of extended aromatic systems in enhancing hydrophobic interactions.

Demethylated amide/amine/piperazine/pyridinamine osthole derivatives

Docking-based assessment of demethylated and nitrogen-enriched osthole derivatives (**89-100**) revealed distinct activity modulation depending on side-chain functionality. The demethylated amide derivatives (**89-92**) exhibited consistent fragrance affinity (-8.17 to -8.99 kcal/mol) with moderate antioxidant (-9.44 to -10.39 kcal/mol), anti-melanogenic (-7.15 to -8.47 kcal/mol), and anti-inflammatory (-6.93 to -8.11 kcal/mol) interactions, indicating stable yet moderate multitarget engagement. Incorporation of amine and piperazine moieties (**93-96**) broadened activity windows, enhancing antioxidant (-10.08 to -11.16 kcal/mol) and anti-melanogenic (-8.40 to -9.44 kcal/mol) potency while maintaining appreciable fragrance (-7.01 to -9.09 kcal/mol) and anti-inflammatory (-7.27 to -9.09 kcal/mol) binding. Notably, pyridinamine derivatives (**97-100**) demonstrated the highest anti-melanogenic affinity (-8.70 to -10.56 kcal/mol) within this set, accompanied by sustained antioxidant activity (-9.29 to -10.57 kcal/mol), suggesting that aromatic nitrogen incorporation improves electronic complementarity with pigmentation-related targets. In addition, these compounds exhibited moderate fragrance receptor binding (-6.46 to -7.70 kcal/mol) and appreciable anti-inflammatory activity (-7.41 to -8.90 kcal/mol). Among the series, derivatives **94**, **97** and **100** exhibited superior combined target affinities (Figure 2). The SAR of this series demonstrates that progressive incorporation of nitrogen-containing functionalities significantly modulates multitarget activity. The demethylated amide derivatives (**89-92**) show moderate activity, where increased hydrophobic bulk (cyclohexane, **90**) enhances antioxidant and anti-melanogenic binding compared to aliphatic substitution **89**, while aromatic substitution **91** further improves anti-melanogenic affinity (-8.47 kcal/mol). Introduction of amine linkage **93**, **94** markedly enhances activity, particularly with halogen substitution (**94**, *o*-Br-Ph), which improves all targets, indicating favorable electronic and hydrophobic interactions. Incorporation of piperazine moieties (**95-97**) shifts activity toward anti-melanogenic targets, with **96** and **97** showing the highest binding, suggesting that increased polarity and multiple nitrogen centres favor enzyme interactions. Compound **97** exhibits pronounced anti-

©Copyright protected. Unauthorised republication, reproduction, distribution, dissemination and copying of this document in whole or in part is strictly prohibited.

melanogenic activity driven by a nitrogen-rich pyridinamine-piperazine scaffold, which enables diverse interaction modes within the tyrosinase active site. Hydrogen bonds provide firm anchoring, while π-cation enhance electrostatic and aromatic stabilization. Concurrent π-alkyl interactions facilitate hydrophobic fitting within non-polar regions (Figure 3). Further variation with heterocyclic amines (**98-100**) maintains balanced activity, where piperidine **100** shows strong antioxidant and anti-melanogenic interactions, while morpholine **98** and pyrrolidine **99** provide moderate multitarget profiles.

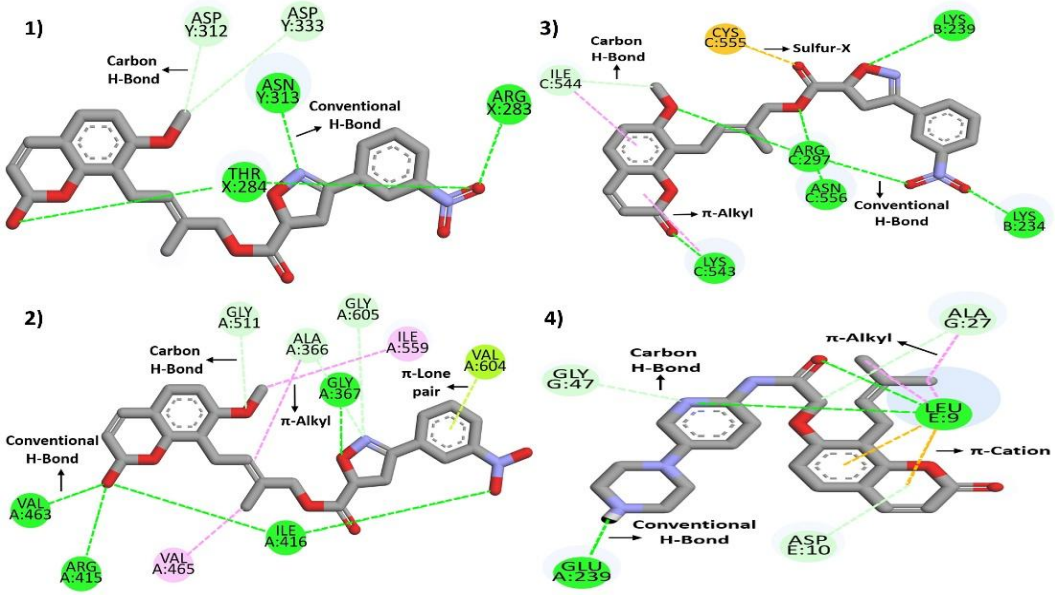

Figure 3: Interactions of top leads within the active site of proteins: osthole-ester (35)-OR51E2 (1); Keap1 (2); Tyr (3), demethylated pyridinamine osthole (97)-Cox2 (4).

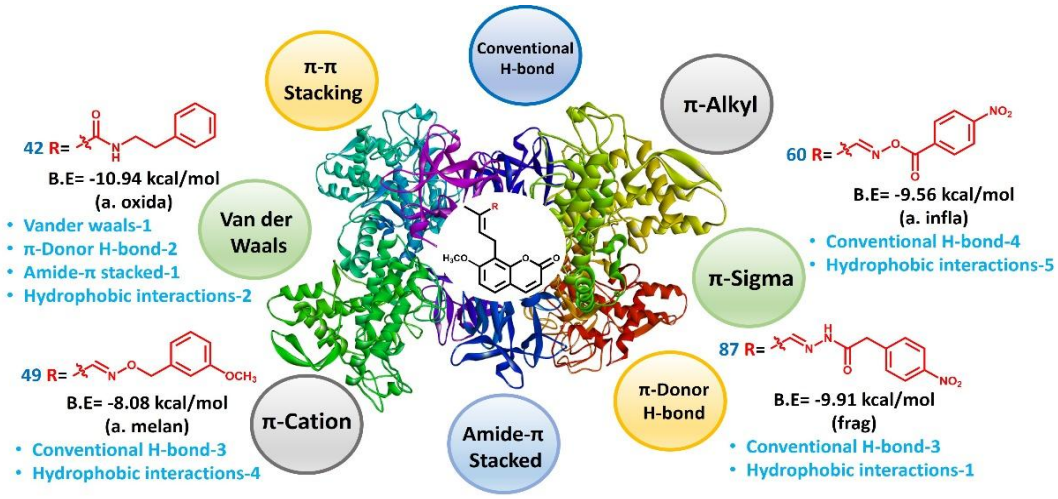

Figure 4: Various stabilizing interactions of some representative compounds.

Overall, the SAR analysis reveals that multitarget activity is governed by a fine balance of structural, electronic and interactional factors. Optimal chain length (2-3 carbons) and linker elongation, combined with partial rigidity through unsaturation and conjugation, significantly enhance binding across targets. Strong electron-withdrawing substituents, particularly nitro (-NO_2) groups especially at the *m*-position along with *p*-halogen substitutions, markedly improve activity by enhancing electronic complementarity and interaction strength, as exemplified by compound **35**, which favours broad multitarget engagement. In contrast, nitrogen-rich heterocyclic substitutions such as in compound **97**, promote stronger enzyme-specific interactions. Moderate electron-donating groups (-OCH_3) and controlled steric effects further contribute to balanced activity. Additionally, oxygen-rich and heteroaromatic systems, along with nitrogen-containing functionalities, enhance interactions with enzyme targets, whereas hydrophobic and halogenated aromatic moieties favor fragrance receptor affinity and anti-inflammatory activity. Importantly, superior multitarget binding is associated with greater interaction diversity, mainly the synergistic combination of conventional and carbon H-bonds with π-based interactions across OR51E2, Keap1, COX-2 and tyrosinase, while substituent electronics and linker flexibility modulate target selectivity and binding efficiency. Derivatives of ester (**2**, **5**, **16**, **22-23**, **25**, **35**), amide (**42**), oxime-ether (**49**, **52**), oxime-ester (**60**, **64**, **66**, **73**),

©Copyright protected. Unauthorised republication, reproduction, distribution, dissemination and copying of this document in whole or in part is strictly prohibited.

acylhydrazone (**83**, **87)**, demethylated amine and pyridinamine (**94**, **97**, **100)** emerge as the most promising derivatives, exhibiting an optimal balance of steric flexibility, electronic tuning, interaction diversity and multitarget binding efficiency (Figure 4). And also, osthole framework leads to enhanced multitarget efficacy, improved pharmacokinetic behaviour and greater therapeutic potential compared to both the parent and conventional reference compounds - galaxolide, butylated hydroxytoluene, methoxsalen and diclofenac.

CONCLUSION

In summary, the present study demonstrates that rational structural modification of the osthole scaffold yields a diverse library of derivatives with well-balanced physicochemical, safety and multitarget functional profiles suitable for cosmeceutical applications such as fragrance, antioxidant, anti-melanogenic and anti-inflammatory properties. The integrated ADME-toxicity assessment confirmed favorable cosmetic-likeness, optimal lipophilicity-polarity balance, controlled skin permeability and excellent safety characteristics across all derivatives. SAR analysis revealed that multitarget efficacy is governed by an interplay of linker length, conformational flexibility, electronic effects and substituent positioning. In particular, moderate chain elongation, incorporation of unsaturation and the presence of strong electron-withdrawing groups significantly enhanced binding affinity across OR51E2, Keap1, COX-2 and tyrosinase, while nitrogen-rich functionalities improved enzyme-specific interactions and solubility profiles. Notably, compounds **35** (ester derivative) and **97** (demethylated pyridinamine derivative) emerged as the top-performing leads, exemplifying optimal electronic tuning, interaction diversity and broad-spectrum target engagement. The most promising candidates-ester, amide, oxime-ether/ester, acylhydrazone and nitrogen-enriched classes exhibited superior interaction diversity and binding efficiency, reflecting their optimized structural features. Collectively, this work establishes that we have validated a series of osthole hybrids for cosmeceutical applications, highlighting their potential as effective, safe and multifunctional candidates for advanced cosmetic formulations in antioxidant, UV defense, anti-inflammatory, pigmentation control and fragrance stabilization.

Author Contributions

DD & AK conceived the study, performed simulations, analyzed data and wrote the manuscript.

Source of Support: The author(s) received no financial support for the research, authorship, and/or publication of this article

Conflict of Interest: The author(s) declared no potential conflicts of interest with respect to the research, authorship, and/or publication of this article.

REFERENCES

1. Beom Kim S, Kim C, Liu Q, Hee Jo Y, Joo Choi H, Hwang BY, Kyum Kim S, Kyeong Lee M, Optimization of extraction conditions for osthol, a melanogenesis inhibitor from Cnidium monnieri fruits, Pharmaceutical Biology, 2016; 54(8):1373-1379. https://doi.org/10.3109/13880209.2015.1078382.
2. Immaculate A, Kalpana A, In Silico Analysis of Flavonoid-Triazole Hybrid Inhibitors Targeting Neurodegenerative, Oncological, and Infectious Diseases, International Journal of Pharmaceutical Sciences Review and Research, 2026; 86(4):139-147. http://dx.doi.org/10.47583/ijpsrr.2026.v86i4.017.
3. Lv M, Ding H, Xu H, Osthole: A Coumarin with Dual Roles in Biology and Chemistry, Biology, 2025; 14(6):588. https://doi.org/10.3390/biology14060588.
4. Morris GM, Goodsell DS, Halliday RS, Huey R, Hart WE, Belew RK, Olson AJ, Automated docking using a lamarckian genetic algorithm and an empirical binding free energy function, Journal of Computational Chemistry, 1988; 19:1639-1662. CCC 0192-8651/98/141639-24.
5. Pettersen EF, Goddard TD, Huang CC, Couch GS, Greenblatt DM, Meng EC, Ferrin TE, UCSF Chimera-a visualization system for exploratory research and analysis, Journal of Computational Chemistry, 2004; 25:1605-1612. https://doi.org/10.1002/jcc.20084.
6. Dassault Systèmes: BIOVIA Discovery Studio Visualizer 2021. Available online: https://discover.3ds.com/discovery-studio visualizer-download (accessed on 15 March 2023).
7. Daina A, Michielin O, Zoete V, SwissADME: a free web tool to evaluate pharmacokinetics drug-likeness and medicinal chemistry friendliness of small molecules, Scientific Reports, 2017; 7:42717. https://doi.org/10.1038/srep42717.
8. Myung Y, De Sá AGC, Ascher DB, Deep-PK: Deep Learning for Small Molecule Pharmacokinetic and Toxicity Prediction, Nucleic Acids Research, 2024; 52:W469-W475. doi:10.1093/nar/gkae254.

For any questions related to this article, please reach us at: globalresearchonline@rediffmail.com
New manuscripts for publication can be submitted at: submit@globalresearchonline.net and submit_ijpsrr@rediffmail.com

©Copyright protected. Unauthorised republication, reproduction, distribution, dissemination and copying of this document in whole or in part is strictly prohibited.